REMOTE SENSING SIGNATURE FIELDS RECONSTRUCTION VIA ROBUST REGULARIZATION OF BAYESIAN MINIMUM RISK TECHNIQUE

***Yuriy V. Shkvarko**, Senior Member, IEEE, **Ivan E. Villalon-Turrubiates**, Member, IEEE, and **Jose L. Leyva-Montiel,** Member, IEEE*

Center of Research and Advanced Studies (CINVESTAV) Campus Guadalajara
Avenida Científica 1145, Colonia El Bajío, 45010, Zapopan Jalisco, México
shkvarko@gdl.cinvestav.mx, villalon@gdl.cinvestav.mx, luis.leyva@cts-design.com

ABSTRACT

The robust numerical technique for high-resolution reconstructive imaging and scene analysis is developed as required for enhanced remote sensing with large scale sensor array radar/synthetic aperture radar. The problem-oriented modification of the previously proposed fused Bayesian-regularization (FBR) enhanced radar imaging method is performed to enable it to reconstruct remote sensing signatures (RSS) of interest alleviating problem ill-poseness due to system-level and model-level uncertainties. We report some simulation results of hydrological RSS reconstruction from enhanced real-world environmental images indicative of the efficiency of the developed method.

Index Terms – Signal processing, system fusion, image reconstruction, regularization.

1. INTRODUCTION

Modern applied theory of reconstructive image processing is now a mature and well developed research field, presented and detailed in many works (see, for example [1] thru [11] and references therein).

Although the existing theory offers a manifold of statistical and descriptive regularization techniques for reconstructive imaging in many application areas there still remain some unresolved crucial theoretical and processing problems related to large scale sensor array real-time reconstructive image processing. In this study, we consider the problem of enhanced remote sensing (RS) imaging and computational reconstruction of remote sensing signature (RSS) fields of the RS scenes with the use of array radars or synthetic aperture radars (SAR) as sensor systems. The major innovative contributions of this study is the development of a robust version of the fused Bayesian-regularization (FBR) method [1], [2] for reconstruction of the power spatial spectrum pattern (SSP) of the wave field scattered from the RS scene and related RSS given a finite set of SAR signal recordings.

2. PROBLEM MODEL

Consider the measurement data wavefield $u(\mathbf{y})=s(\mathbf{y})+n(\mathbf{y})$ modeled as a superposition of the echo signals s and additive noise n that assumed to be available for observations and recordings within the prescribed time-space observation domain $Y \ni \mathbf{y}$, where $\mathbf{y}=(t,\mathbf{p})^{\mathrm{T}}$ defines the time-space points in the observation domain $Y=T\times P$. The model of observation wavefield u is specified by the linear stochastic equation of observation (EO) of operator form [2]: $u=Se+n$; $e\in \mathrm{E}$; $u,n\in \mathrm{U}$; $S:\mathrm{E}\to\mathrm{U}$. The RS imaging problem is stated as follows: to find an estimate $\hat{B}(\mathbf{x})$ of the SSP $B(\mathbf{x})$ in the environment $X \ni \mathbf{x}$ by processing whatever values of measurements of the data wavefield $u(\mathbf{y})$; $\mathbf{y}\in Y$, are available.

Following the RS methodology [2], [3], any particular physical RSS of interest is to be extracted from the reconstructed RS image $\hat{B}(\mathbf{x})$ applying some specified signature extraction operator Λ [4].

The particular RSS is mapped applying Λ to the reconstructed image, i.e.

$$\hat{\Lambda}(\mathbf{x})=\Lambda(\hat{B}(\mathbf{x}))\,. \qquad (1)$$

Last, taking into account the RSS extraction model of Eq. (1), we can reformulate now the signature reconstruction problem as follows: to map the reconstructed particular RSS of interest $\hat{\Lambda}(\mathbf{x})=\Lambda(\hat{B}(\mathbf{x}))$ over the observation scene $X \ni \mathbf{x}$ via post-processing whatever values of the reconstructed scene image $\hat{B}(\mathbf{x})$; $\mathbf{x}\in X$ are available.

3. GENERALIZATION OF THE FBR METHOD

The estimator that produces the optimal estimate $\hat{\mathbf{B}}$ of the SSP vector via processing the M-D data recordings applying the FBR estimation strategy that incorporates nontrivial a priori geometrical and projection-type model information was developed in our previous study [1].

Such optimal FBR estimate is given by the nonlinear equation

$$\hat{\mathbf{B}} = \mathbf{B}_P + \mathbf{P}\mathbf{B}_0 + \mathbf{W}(\hat{\mathbf{B}})(\mathbf{V}(\hat{\mathbf{B}}) - \mathbf{Z}(\hat{\mathbf{B}})) . \quad (2)$$

In Eq. (2), $\mathbf{B}_0$ represents the a priori SSP distribution to be considered as a zero step approximation to the desires SSP $\hat{\mathbf{B}}$.

Note that in this study, we use all the notations from [1] for definitions of the sufficient statistics (SS) vector $\mathbf{V}(\hat{\mathbf{B}}) = \{\mathbf{F}(\hat{\mathbf{B}})\mathbf{U}\mathbf{U}^{+}\mathbf{F}^{+}(\hat{\mathbf{B}})\}_{\text{diag}}$, the solution-dependent SS formation operator

$$\mathbf{F} = \mathbf{F}(\hat{\mathbf{B}}) = \mathbf{D}(\hat{\mathbf{B}})(\mathbf{I} + \mathbf{S}^{+}\mathbf{R}_{\mathbf{N}}^{-1}\mathbf{S}\mathbf{D}(\hat{\mathbf{B}}))^{-1}\mathbf{S}^{+}\mathbf{R}_{\mathbf{N}}^{-1} ; \quad (3)$$

the SS shift vector $\mathbf{Z}(\hat{\mathbf{B}}) = \{\mathbf{F}(\hat{\mathbf{B}})\mathbf{R}_{\mathbf{N}}\mathbf{F}^{+}(\hat{\mathbf{B}})\}_{\text{diag}}$, and the composite solution-dependent smoothing-projection window operator

$$\mathbf{W}(\hat{\mathbf{B}}) = \mathbf{P}\boldsymbol{\Omega}(\hat{\mathbf{B}}) \quad (4)$$

with the projector

$$\mathbf{P} = (\mathbf{I} - \mathbf{G}^{-}\mathbf{G}) \quad (5)$$

and the solution-dependent regularizing window

$$\boldsymbol{\Omega}(\hat{\mathbf{B}}) = (\text{diag}(\{\mathbf{S}^{+}\mathbf{F}^{+}\mathbf{F}\mathbf{S}\}_{\text{diag}}) + \alpha\mathbf{D}^{2}(\hat{\mathbf{B}})\mathbf{M}(\hat{\mathbf{B}}))^{-1} , \quad (6)$$

in which the regularization parameter α is to be adaptively adjusted using the system calibration data [1].

The generalization of the FBR estimator of Eq. (2) for the case of RSS reconstruction in the K-D solution space can now be performed taking into account the pixel format of the basis $\{g_k(\mathbf{x})\}$ spanning the RSS solution space that yields

$$\hat{\Lambda}_{(K)}(\mathbf{x}) = \sum_{k=1}^{K} \Lambda(\hat{B}_k) |g_k(\mathbf{x})|^2 ; \quad \mathbf{x} \in X . \quad (7)$$

Hence, in the adapted pixel-format solution space, the vector $\hat{\Lambda} = \boldsymbol{\Lambda}(\hat{\mathbf{B}})$ composed of pixels $\{\Lambda(\hat{B}_k); k=1,\ldots,K\}$ represents the desired pixel-format map of the high-resolution RSS reconstructed over the observed scene.

Because of the complexity of the solution-dependent K-D operator inversions needed to be performed to compute the SS, $\mathbf{V}(\hat{\mathbf{B}})$, and the window, $\mathbf{W}(\hat{\mathbf{B}})$, the computational complexity of such generalized optimal algorithm of Eq. (7) is extremely high. Hence, the Eq. (7) can not be addressed as a practically realizable estimator of the RSS.

4. ROBUSTIFIED FBR TECHNIQUE

Here we propose the robustification scheme for quasi-real-time implementation of the generalized FBR estimator (7) that reduces drastically the computation load of the RSS formation procedure without substantial degradation in the SSP resolution and overall RSS map performances.

We propose the robust version of the FBR estimator (referred to as RFBR method) via roughing $\mathbf{P}=\mathbf{I}$ and performing the robustification of both the SS formation operator $\mathbf{F}(\hat{\mathbf{B}})$ and the smoothing window $\boldsymbol{\Omega}(\hat{\mathbf{B}})$ in Eq. (2) by roughing $\mathbf{D}(\hat{\mathbf{B}}) \approx \mathbf{D} = \beta\mathbf{I}$, where β represents the expected a priori image gray level [1]. Thus, the robust SS formation operator

$$\mathbf{F} = \mathbf{A}^{-1}(\rho)\mathbf{S}^{+} \quad \text{with} \quad \mathbf{A}(\rho) = \mathbf{S}^{+}\mathbf{S} + \rho^{-1}\mathbf{I} \quad (8)$$

becomes an inverse of the SFO $\mathbf{S}$ with regularization parameter ρ^{-1}, the inverse of the signal-to-noise ratio (SNR) $\rho = \beta / N_0$ for the adopted white observation noise model, $\mathbf{R}_{\mathbf{N}} = N_0\mathbf{I}$.

The robust smoothing window

$$\mathbf{W} = \boldsymbol{\Omega} = (w_0\mathbf{I} + \mathbf{M})^{-1} \quad (9)$$

is completely defined now by matrix $\mathbf{M}$ that induces the metric structure in the solution space with the scaling factor $w_0 = \text{tr}\{\mathbf{S}^{+}\mathbf{F}^{+}\mathbf{F}\mathbf{S}\}/K$ [2].

Note that such robustified $\mathbf{W}$ can be pre-computed a priori for a family of different admissible ρ as it was performed in the previous studies [1], [2].

Here, we adopt practical constraints of high SNR operational conditions [5], [6] $\rho >> 1$, in which case one can neglect also the constant bias $\mathbf{Z} = Z_0\mathbf{I}$ in Eq. (2) because it does not affect the pattern of the SSP estimate.

Following these practically motivated assumptions, the resulting RFBR estimator is

$$\hat{\Lambda}_{RFBR}(\mathbf{x}) = \mathbf{g}^{\mathrm{T}}(\mathbf{x})\text{diag}(\Lambda(\mathbf{B}_0 + \boldsymbol{\Omega}\mathbf{V}))\mathbf{g}(\mathbf{x}) \quad (10)$$

where $\mathbf{V} = \{\mathbf{F}\mathbf{U}\mathbf{U}^{+}\mathbf{F}^{+}\}_{\text{diag}}$ represents now the robust (solution independent) SS vector.

The principal computational load of the RFBR estimator of Eq. (10) is associated now with the operator inversions required to compute the solution operator of Eq. (9) for adaptively adjusted regularization parameter ρ^{-1}.

Next, the simplest rough RSS estimator can be constructed as further simplification of Eq. (10) adopting the trivial prior model information ($\mathbf{P}=\mathbf{I}$ and $\mathbf{B}_0 = 0\mathbf{I}$) and roughly approximation the SS formation operator $\mathbf{F}$ by the adjoint SFO, i.e. $\mathbf{F} \approx \gamma_0\mathbf{S}^{+}$ [1].

In this case, the Eq. (10) is simplified to its rough version

$$\hat{\Lambda}_{MSF}(\mathbf{x}) = \mathbf{g}^{\mathrm{T}}(\mathbf{x})\text{diag}(\Lambda(\boldsymbol{\Omega}\mathbf{H}))\mathbf{g}(\mathbf{x}) \quad (11)$$

referred to as matched spatial filtering (MSF) algorithm where the rough SS $\mathbf{H} = \gamma_0^2\{\mathbf{S}^{+}\mathbf{U}\mathbf{U}^{+}\mathbf{S}\}_{\text{diag}}$ is now formed applying the adjoint operator $\mathbf{S}^{+}$, and the windowing of the rough SS is performed applying the smoothing filter $\boldsymbol{\Omega} = (w_0\mathbf{I} + \mathbf{M})^{-1}$ with nonnegative entry, the same one as was constructed numerically in [1].

a. Original super-high resolution scene

b. Low-resolution image formed with the MSF

c. Scene image reconstructed with the R-FBR method

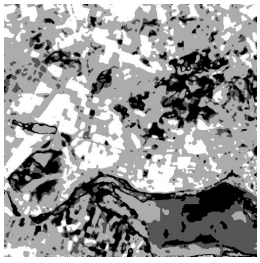

d. HEM extracted from the original scene

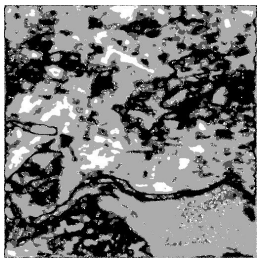

e. HEM extracted from the MSF image

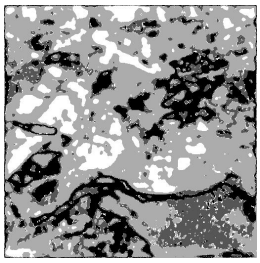

f. HEM extracted from the R-FBR reconstructed image

Figure 1. Simulation results for the first operation scenario

a. Original super-high resolution scene

b. Low-resolution image formed with the MSF

c. Scene image reconstructed with the R-FBR method

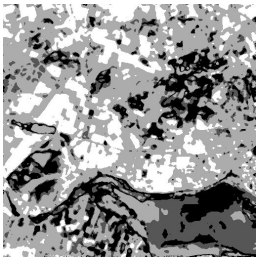

d. HEM extracted from the original scene

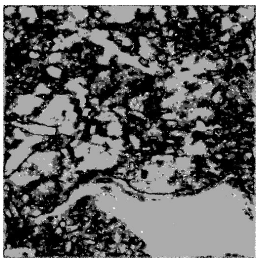

e. HEM extracted from the MSF image

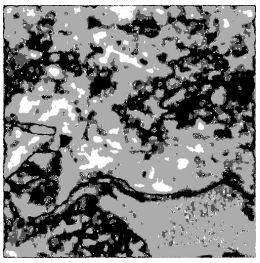

f. HEM extracted from the R-FBR reconstructed image

Figure 2. Simulation results for the second operation scenario

5. SIMULATIONS

In the simulations, we considered the SAR with partially (fractionally) synthesized aperture as an RS imaging system [7], [8]. The SFO was factorized along two axes in the image plane: the azimuth (horizontal axis) and the range (vertical axis).

Following the common practically motivated technical considerations [6], [7], [9] we modeled a triangular shape of the SAR range ambiguity function of 3 pixels width, and a $|sinc|^2$ shape of the side-looking SAR azimuth ambiguity function (AF) for two typical scenarios of fractionally synthesized apertures: (i) azimuth AF of 10 pixels width at the zero crossing level associated with the first system model and (ii) azimuth AF of 20 pixels width at the zero crossing level associated with the second system model, respectively.

The RS scenes are borrowed from the real-world RS imagery of the Metropolitan area of Guadalajara city in Mexico [10], [11].

Figures 1.a. and 2.a show the original super-high resolution test scenes.

Figures 1.b and 2.b present scene images formed with the conventional MSF algorithm of Eq. (11).

Figures 1.c and 2.c present the SSP reconstructed applying the proposed RFBR method of Eq. (10).

The particular reconstructed RSS reported in the simulations in Figures 1.(d,e,f) and 2.(d,e,f) represent the so-called hydrological electronic maps (HEMs) [3], [4] extracted from the relevant SSP images applying the weighted order statistics (WOS) classification operator $\Lambda(\hat{B}(\mathbf{x}))$ detailed in [4].

Such HEMs are specified as 2-bit hydrological RSS [3], [4] that classify the areas in the reconstructed scene images $\hat{B}(\mathbf{x})$ into four classes: areas covered with water (black zones in the figures), the high-humidity areas (dark-gray zones), the low-humidity areas (light-gray zones), and dry areas/non classified regions (white zones).

Table 1. IOSNR values provided with the R-FBR method. Results are reported for different SNRs for two different simulated SAR systems

SNR [dB]	*IOSNR* First System		*IOSNR* Second System	
μ	*SSP*	*HEM*	*SSP*	*HEM*
10	2.35	2.24	2.42	3.20
15	5.15	3.34	5.56	4.32
20	8.24	5.20	8.72	5.12
25	17.54	13.48	17.91	14.89

The quantitative measure of the improvement in the output signal-to-noise ratio (*IOSNR)* quality metric [7] gained with the enhanced SSP and HEM imaging methods for two simulated scenarios are reported in Table 1. All reported simulations were run for the same 512x512 pixel JPEG image format. The computation load of the enhanced RSS reconstruction with the RFBR algorithm (10) applying the proposed computational scheme in comparison with the original FBR method (7) was decreased approximately 10^5 times and required 0.38 seconds of the overall computational time using a personal computer with a 2.8GHz Pentium4© processor and 512MB of random access memory (RAM).

6. CONCLUDING REMARKS

We have developed and presented the RFBR method for high-resolution SSP estimation and RSS mapping as required for reconstructive RS imagery although it may also be applied to other fields. The developed technique performs the balanced aggregation of the data and model prior information to perform the enhanced image reconstruction and RSS mapping with improved spatial resolution and noise reduction. The presented simulation examples illustrate the overall imaging performance improvements gained with the proposed approach. The simulation experiment verified that the RSS extracted applying the RFBR reconstruction method provide more accurate physical information about the content of the RS scenes in comparison with the conventional MSF and previously proposed descriptive regularization techniques [2], [4], [10].

The presented study establishes the foundation to assist in understanding the basic theoretical and computational aspects of multi-level adaptive RS image formation, enhancement and extraction of physical scene characteristics. The study was undertaken in a context of RS data processing as required for large scale SAR imagery and RS scene analysis, although, the results can be extended to other research areas in intelligent sensor systems design and applications.

7. REFERENCES

[1] Y.V. Shkvarko, "Estimation of Wavefield Power Distribution in the Remotely Sensed Environment: Bayesian Maximum Entropy Approach", *IEEE Transactions on Signal Processing*, vol. 50, 2002, pp. 2333-2346.

[2] Y.V. Shkvarko and I.E. Villalon-Turrubiates, "Unified Bayesian-Experiment Design Regularization Technique for High-Resolution of the Remote Sensing Imagery", *Proceedings of the 1st IEE International Workshop on Computational Advances in Multi-Sensor Adaptive Processing*, IEEE Press, Puerto Vallarta, 2005, pp. 165-168.

[3] *Principles and Applications of Imaging Radar*, F.M. Henderson and A.V. Lewis, Ed., *Manual of Remote Sensing*, 3d Edition, Vol. 3 , John Willey and Sons Inc., New York, 1998.

[4] S.W. Perry, H.S. Wong and L. Guan, *Adaptive Image Processing: A Computational Intelligence Perspective*, CRC Press: New York, 2002.

[5] S.E. Falkovich, V.I. Ponomaryov, and Y.V. Shkvarko, *Optimal Reception of Space-Time Signals in Radio Channels With Scattering*, Radio i Sviaz, Moscow, 1989.

[6] D.R. Wehner, *High-Resolution Radar*, 2nd edn, Artech House: Boston, 1994.

[7] Y.V. Shkvarko, "Unifying Regularization and Bayesian Estimation Methods for Enhanced Imaging with Remotely Sensed Data. Part II – Implementation and Performance Issues", *IEEE Transactions on Geoscience and Remote Sensing*, vol. 42, 2004, pp. 932-940.

[8] G. Franceschetti, A. Iodice, S Perna, and D. Riccio, "Efficient Simulation of Airborne SAR Raw Data of Extended Scenes", *IEEE Transactions on Geoscience and Remote Sensing,* vol. 44, No. 10, pp. 2851-2860, Oct. 2006.

[9] V.I. Ponomaryov and L. Nino-de-Rivera, "Order Statistics, M Method in Image and Video Sequence Processing Applications", *Journal on Electromagnetic Waves and Electronic Systems*, vol. 8, Moscow, 2003, pp. 99-107.

[10] Y.V. Shkvarko and I.E. Villalon-Turrubiates, "Dynamical Enhancement of the Large Scale Remote Sensing Imagery for Decision Support in Environmental Resource Management", *Proceedings of the 18th Information Resource Management Association International Conference*, Idea Group Inc, Vancouver, 2007.

[11] Space Imaging, *http://www.spaceimaging.com/quicklook*, GeoEye Inc., 2007.